

# Effect of nitrogen doping and tunable pore structures on arsenic removal

Jisun Han, Daegwon Ha and Shinhoo Kang\*

\*Department of Materials Science and Engineering, Seoul National University, Seoul, 151-742, Korea

## ABSTRACT

Nitrogen doped carbons were synthesized by a carbo-nitride derived carbon (CNDC) at various chlorination temperatures. CN73s that have both small micro- and meso-pores with nitrogen functional group, such as pyrrolic-N at the surface of pores, show excellent adsorption ability for the arsenic complex ions. Experimental and theoretical calculation results suggested that pore structure and the types of nitrogen functional groups making the CN73s highly charged significantly influenced the adsorption of arsenic. The small micro-pores(0.7 nm) that pyrrolic-N is placed at the edge of pores are active sites for capturing arsenic complex ions. The small meso-pores provide the diffusion path for arsenic ions and enhance the adsorption kinetics.

**Keywords:** arsenic adsorption, nitrogen doped porous carbon, carbo-nitride derived carbon (CNDC), pore size distribution, nitrogen functional groups

## 1 INTRODUCTION

The arsenic and its compound are highly toxic and some of them are carcinogen. They could spread into ground water through geothermal, mining and industrial activity, and contaminate ground water. A large amount of water resources around the world contain significant concentration of arsenic ranged from 0.5 to 5000  $\mu\text{g/L}$ . To secure drinking water, removal of arsenic is vitally required. Therefore, developing adsorption material and elimination technology became a big global issue and numerous studies are currently underway.

The porous carbons, especially carbide derived carbon (CDC), synthesized by a chlorination of various carbides is one of the typical adsorbent materials. CDC has well developed pore structure not only on its surface but also in bulk [1]. Thus, it is widely applied as the substrate for the gas adsorption and the electrochemistry application [2, 3]. Particularly, certain size of micro-pores and small meso-pores are uniformly formed in CDC via controlling experimental factors [4]. It is suitable for small sized gas adsorption such as hydrogen, carbon dioxide. Because micro-pores, which could catch gas molecules via overlapping of interaction force between the pore walls, act as adsorption sites and meso-pores provide the kinetic path to gas molecules enhancing diffusion of gas molecules within the bulk of CDC [5].

Meanwhile, pure porous carbon itself has high stability and is electrically neutralized. Therefore, it has low van der

Waals interaction (4 kJ/mol) with gas molecules or electrolytes. To enhance the interaction energy, hetero atom doping is extensively implemented notably the nitrogen. A number of research about nitrogen doped carbons are currently in progress. Thus nitrogen doped carbons are widely applied as adsorbent, electrode for energy storage device and catalyst for electrochemical applications [6, 7].

In this paper, N-doped porous carbon was synthesized by a carbo-nitride derived carbon (CNDC), which is similar to the CDC process. It has both micro-pores and meso-pores which is the advantage of CDC. Furthermore, the nitrogen is successfully doped on edges of CNDC along with pore development. Therefore, aforementioned N-doped porous carbon has the positively charged surface that could enhance the adsorption ability for arsenic ions in water. This material shows outstanding adsorption performance for arsenic compared with other carbon materials. Also, its performance is comparable to metal oxide adsorbents, such as iron oxide, aluminium oxide, commonly used in arsenic removal. We denoted entire samples as CN73s and each sample as CN-X; In CN73s, 73 represents the carbon-to-nitrogen ratio of the  $\text{Ti}(\text{C}_7\text{N}_3)$  precursors. X signifies the chlorination temperature.

## 2 RESULTS AND DISCUSSION

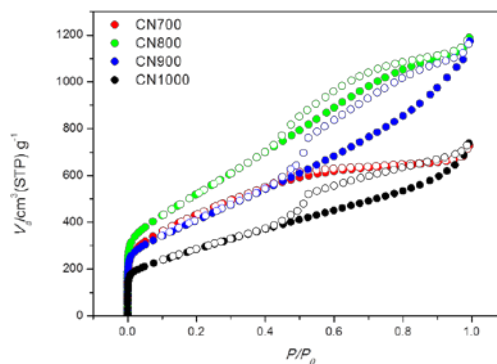


**Figure 1:  $\text{N}_2$  sorption isotherms of CN73s (solid – adsorption, open – desorption)**

The  $\text{N}_2$  sorption isotherms, shown in fig. 1, exhibit the pore structure of CN73s. CN700 have type I isotherm with mild slope of  $P/P_0 = 0.1\sim 0.5$ , which represents the development of micro-pores wider than those of pure micro-porous materials like typical CDC. The sorption isotherms of pure CDC usually have sharp hill at low relative pressure and plateau over wide ranges. TiC-CDC, as a typical CDC, have negligible meso-pores but above

1200°C, hysteresis loop begins to appear representing meso-pores [8]. However porous CN73s, chlorinated from nitrogen substituted TiC, well develops meso-region pores from synthesis temperature of 800°C. Its sorption isotherms change into Type H3 and H4 hysteresis loops between 800~1000°C, which represent aggregations of narrow meso-pores [9]. CN73s, with similar pore forming agent like CDC, developed pore structure well with more than 1000 m<sup>2</sup>/g surface area calculated by Brunauer-Emmett-Teller (BET) model. CN800 and CN900 have large amount of N<sub>2</sub> adsorption especially for meso-region whereas CN1000 decreases its N<sub>2</sub> adsorption by partial collapse of the pore network with longer graphitic layers growing. According to pore characteristics, CN800 showed highest values in micro- and meso- pore volumes among the CN73s. Surface area of CN1000 significantly decreased as its micro- and meso-pore volumes decrease, and it is caused by growth of pore width, which is influenced by curved graphitic layers. The textural properties are summarized in Table 1.

The pore size distribution (PSD) of CN73s, calculated by non-local density functional theory (NLDFT), are broadened by increasing the chlorination temperature displayed in fig. 3. Pores of CN700 are centered at 0.7nm, which is a characteristics of TiC-derived carbon, 1.5nm and 3nm, which is believed to be affected by CN<sub>x</sub> desorption [10]. It has uniform tri-modal distributions, verified as parallel line (figure.1) at P/P<sub>0</sub> = 0.5~0.9 [11]. As synthesis temperature increase, 0.7nm and 1.5nm pores collapsed due to releasing a highly stressed and curved graphitic layers, and it caused the irregularity. Large pores with 20~100nm are well developed in CN1000 while total pore volumes decreased.

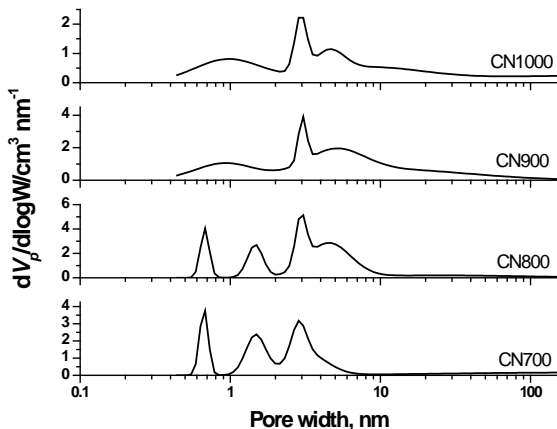


**Figure 2: Pore size distributions (PSD) of CN73s calculated by NLDFT (cylinder pore model).**

X-ray photoelectron spectroscopy (XPS) spectra (figure. 4a) was employed to compare chemical composition and bonding nature of CN73s with different chlorination temperature and summarized in table 2. The CN700,

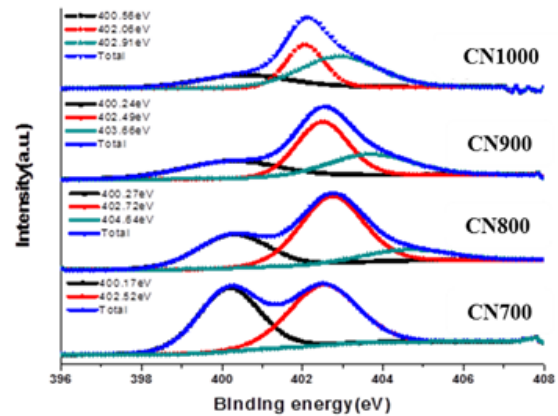


**Figure 3: XPS of N1s spectra of CN37s**

CN800, CN900, and CN1000 possess 3.14, 3.72, 2.67 and 2.17 wt.% nitrogen doping contents, respectively. Nitrogen doping can be divided into two types of configuration as pyrrolic-N (400.37±0.2eV) and oxidized-N (402~404eV), especially N-oxides of pyridinic-N (402.06±0.3eV). Since these functional groups are invariably located at the edges sites [12], the edges caused by pore development can be advantages of such selective doping site [13]. Consequentially, Edges along the pore growth of the whole seem to be a desired sites for an edged-nitrogen doping, given the report which proposes that pores in CDC are developed not only at the surface and throughout the bulk [1]. Micro-sized pores are formed in pure carbide systems but micro- and meso-pores are well developed in carbonitride systems. Pores grow over by decomposing unstable C-N bonding, such as pyrrolic-N (5-membered ring) while stable nitrogen, such as pyridinic- or graphitic-N (6-membered ring), remain or unstable one converted to stable one on the pores [14]. Pyrrolic-N is well developed in CN700 but it decreases dramatically with temperature. Pyridinic-N of all CN73s transforms into N- oxidizes of pyridinic-N on the surface [12].

Adsorption isotherm of arsenic is shown by figure 4. CN900 and CN1000 is incapable of adsorbing arsenic significantly, whereas CN700 and CN800 show strong adsorption behavior. The maximum adsorption values (q<sub>m</sub>) of arsenic are 31.08 and 30.34 mg/g, respectively. The adsorption isotherm for CN73s fits the Langmuir equation which is marked on (Eq. (1)).

$$q = \frac{q_m K_a C}{1 + K_a C} \quad (1)$$

q<sub>m</sub> is the maximum mass adsorbed at saturation conditions per mass unit of adsorbent (mg/g). C is equilibrium aqueous concentration (mg/L) and K<sub>a</sub> is the empirical constant with units of inverse of concentration C (/mg)

Through the above experimental results, it is estimated that the optimized pore-structure and nitrogen functional groups located on the surface of pores are the key factors

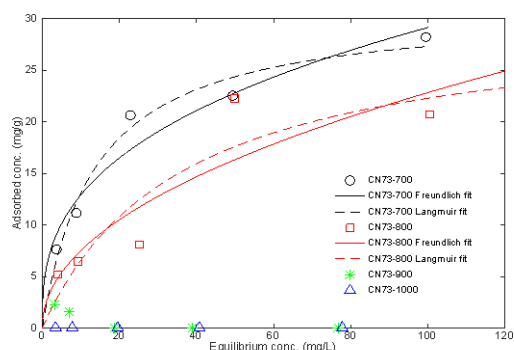


**Figure 4: Adsorption isotherm of As on CN73s (700, 800, 900 and 1000 °C)**

for adsorption of arsenic. Based on the PSD of CN73s and the arsenic adsorption isotherm, small micro-pores (0.7 nm) provide the active sites for adsorbing the arsenic ions. CN900 and CN1000 that small micro-pores are barely developed could not adsorb the arsenic. On the other hand, CN700 and CN800 have tri-modal pore distribution showing small micro-pore(0.7 nm), big micro-pore(1.5 nm) and meso -pore(3.0nm) are harmoniously developed. Thus, through the small micro-pores, they could effectively capture the arsenic and meso-pores could be the kinetic path that enhances the diffusion of the arsenic ions to interior of CN700 and CN800. The advantage of bio-modal pore size distribution that both micro- and meso-pores are simultaneously developed is verified and widely applied to gas adsorption and electrochemistry field [5]. Not only the pore structure but also the nitrogen functional group, especially pyridinic-N could be important for arsenic adsorption. Based on the XPS results, as mentioned above, CN700 and CN800 contain considerable amount of pyrrolic-N and N-oxides of pyridinic-N. In contrast, pyrrolic-N nearly vanished and only N-oxides of pyridinic-N are dominant in the case of CN900 and 1000. Therefore, it is estimated that optimized pore-structure that both micro-pores and meso-pores are well developed and pyrrolic-N located on the surface of pores are the key factors for adsorption of arsenic.

To identify the interaction that works on between arsenic ions and nitrogen doped carbons, we calculate optimized structures and binding strengths of As complex on adsorption sites which are chosen based on the XPS spectrums in figure 3. Four water molecules surrounding As

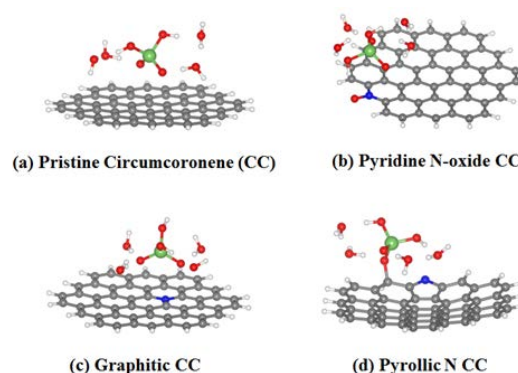


**Figure 5: Optimized adsorbed structure of As complex, H<sub>2</sub>AsO<sub>4</sub>, and four water molecule on four adsorbents.**

complex are included to mimic aqueous environment. Since adsorbate consists of As complex, H<sub>2</sub>AsO<sub>4</sub>, and four water molecule, zero-point energy and entropy effects are also included. Therefore, binding strength is evaluated from the difference of gibbs free energy before and after reaction, which is defined as  $\Delta G = G_{\text{adsorbent+adsorbate}} - (G_{\text{adsorbate}} + G_{\text{adsorbent}})$ . Each term represent gibbs free energies of corresponding systems and T\*S (temperature \* entropy) term in gibbs free energies are obtained at temperature 25°C. Four N-containing structures (pyridine N-Oxide, graphitic N, and pyrrolic N) and N-free (Pristine) structure shown in figure s1k are examined. The change of gibbs free energies for adsorption on four structures are summarized in table 1k and optimized structures after adsorption are given in figure 1k. It is shown that optimized structures that As complex can be adsorbed on graphitic N and pyrrolic N structure through ionic and covalent bonding, respectively. This result accurately matches with our experimental consequence as we mentioned above. Therefore, the most crucial factors for aresnic adsorption are both pore-structure and nitrogen funtional group located on the edge of pores. The micro-pores that possessed the nitrogen functional goup, such as pyrrolic-N and graphitic-N could effectively captured the arsenics ion because their surface was negaively charged. The small mese-pores(2-10 nm) well developed through the bulk act as the diffusion path for arsenic ion and improve the aresenic adsorption behavior of CN73s.

**Table 1: Pore characteristics of synthesized CN73s at different temperature.**

Samples	SSA (m <sup>2</sup> /g)	Total pore Volume (cm <sup>3</sup> /g)	Micro pore Volume (cm <sup>3</sup> /g)	Meso pore Volume (cm <sup>3</sup> /g)	Mean pore diameter (nm)
CN700	1572.3	1.1137	0.5594	0.4739	2.8332
CN800	1922.8	1.8309	0.6642	1.0734	3.8088
CN900	1496.2	1.7923	0.5284	1.1032	4.7916
CN1000	1037.3	1.1349	0.3677	0.6284	4.3762

**Table 2: The changes of gibbs free energy when As complex surrounded with four water molecules on each adsorbent (Pristine CC, Pyridine N-Oxide CC, Graphitic N CC, and Pyrrolic N CC). Arsenic complex with four water molecules can bind to selective N-containing sites.**

Adsorbent	$\Delta G$ (eV)
Pristine CC	0.36
Pyridine N-Oxide CC	2.71
Graphitic N	-1.72
Pyrrolic N	-1.95

### 3 CONCLUSION

In summary, nitrogen-doped carbons (CN73s) were synthesized through the chlorination of the carbo-nitride material. Both micro- and meso-pores were well developed in CN73s because unstable C-N bond, such as pyrrolic-N contained in CN73s induced pores growing. Among the CN73s, CN700 and CN800 have an extraordinary capacity for arsenic complex adsorption compared to other carbon adsorbents. The maximum arsenic adsorption values ( $q_m$ ) for those materials are measured as 31.08 and 30.34 mg/g, respectively. It is worth noting that the most crucial factors for arsenic adsorption are both pore-structure and nitrogen functional group located on the edge of pores. It is shown through the experiment and the theoretical calculation that the micro-pores which possessed the nitrogen functional groups, especially pyrrolic-N and graphitic-N, could act as active sites for capturing arsenic ions. In addition, the meso-pores developed through the whole bulk of CN73s offered the kinetic path for arsenic ions and enhanced the accessibility to micro-pores located on the inner side of CN73s. To understand the role of pore-structures and nitrogen functional group for arsenic adsorption mechanism in nitrogen-doped carbons more deeply, additional study is highly necessary.

### REFERENCES

[1] GOGOTSI, Y., NIKITIN, A., YE, H., ZHOU, W., FISCHER, J. E., YI, B., FOLEY, H. C. and BARSOUM, M. W. "Nanoporous carbide-derived carbon with tunable pore size". *Nat Mater*, 2, 591-4. 2003

[2] PRESSER, V., MCDONOUGH, J., YEON, S.-H. and GOGOTSI, Y. "Effect of pore size on carbon dioxide sorption by carbide derived carbon". *Energy & Environmental Science*, 4, 3059. 2011

[3] CHMIOLA, J., YUSHIN, G., GOGOTSI, Y., PORTET, C., SIMON, P. and TABERNA, P.-L. "Anomalous increase in carbon capacitance at pore sizes less than 1 nanometer". *Science*, 313, 1760-1763. 2006

[4] YUSHIN, G., DASH, R., JAGIELLO, J., FISCHER, J. E. & GOGOTSI, Y. "Carbide Derived Carbons: Effect of Pore Size on

Hydrogen Uptake and Heat of Adsorption". *Advanced Functional Materials*, 16, 2288-2293. 2006

[5] ROSE, M., KORENBLIT, Y., KOCKRICK, E., BORCHARDT, L., OSCHATZ, M., KASKEL, S. and YUSHIN, G. "Hierarchical micro- and mesoporous carbide-derived carbon as a high performance electrode material in supercapacitors". *Small*, 7, 1108-17. 2011

[6] QIE, L., CHEN, W. M., WANG, Z. H., SHAO, Q. G., LI, X., YUAN, L. X., HU, X. L., ZHANG, W. X. and HUANG, Y. H. "Nitrogen-doped porous carbon nanofiber webs as anodes for lithium ion batteries with a superhigh capacity and rate capability". *Adv Mater*, 24, 2047-50. 2012

[7] WEI, J., ZHOU, D., SUN, Z., DENG, Y., XIA, Y. and ZHAO, D. "A Controllable Synthesis of Rich Nitrogen-Doped Ordered Mesoporous Carbon for CO<sub>2</sub> Capture and Supercapacitors". *Advanced Functional Materials*, 23, 2322-2328. 2013

[8] SILVESTRE-ALBERO, A., RICO-FRANC S, S., RODR GUEZ-REINOSO, F., KERN, A. M., KLUMPP, M., ETZOLD, B. J. M. & SILVESTRE-ALBERO, J. "High selectivity of TiC-CDC for CO<sub>2</sub>/N<sub>2</sub> separation". *Carbon*, 59, 221-228. 2013

[9] SING, K. S. "Reporting physisorption data for gas/solid systems with special reference to the determination of surface area and porosity (Recommendations 1984)". *Pure and applied chemistry*, 57, 603-619. 1985

[10] SEO, M. S., KIM, J. H., KIM, J. M., HAN, J. S., KANG, S., IHM, J. S. and KIM, D. O. "Tunable and selective formation of micropores and mesopores in carbide-derived carbon". *Carbon*, 60, 299-306. 2013

[11] INAGAKI, S., GUAN, S., FUKUSHIMA, Y., OHSUNA, T. and TERASAKI, O. "Novel mesoporous materials with a uniform distribution of organic groups and inorganic oxide in their frameworks". *Journal of the American Chemical Society*, 121, 9611-9614. 1999

[12] LAI, L., POTTS, J. R., ZHAN, D., WANG, L., POH, C. K., TANG, C., GONG, H., SHEN, Z., LIN, J. and RUOFF, R. S. "Exploration of the active center structure of nitrogen-doped graphene-based catalysts for oxygen reduction reaction". *Energy & Environmental Science*, 5, 7936. 2012

[13] PALANISELVAM, T., AIYAPPA, H. B. and KURUNGOT, S. "An efficient oxygen reduction electrocatalyst from graphene by simultaneously generating pores and nitrogen doped active sites". *Journal of Materials Chemistry*, 22, 23799. 2012

[14] PELS, J., KAPTEIJN, F., MOULIJN, J., ZHU, Q. and THOMAS, K. "Evolution of nitrogen functionalities in carbonaceous materials during pyrolysis". *Carbon*, 33, 1641-1653. 1995

\* Address correspondence to [shinkang@snu.ac.kr](mailto:shinkang@snu.ac.kr)